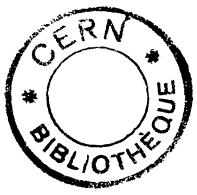

CERN/PS/89-61 (PO)
October 1989

THE 200 kJ PULSER AND POWER CONVERTER FOR THE 36 mm LITHIUM LENS OF THE ANTIPROTON ACCUMULATOR AND COLLECTOR (AAC) AT CERN

F. Voelker

ABSTRACT

Following a short review of the requirements, the lithium-lens pulser and its power converter are described. The design criteria are discussed with regard to the most interesting technical aspects.

CONTENTS

	Page
1. INTRODUCTION	4
2. PERFORMANCE REQUIREMENTS	4
3. CIRCUIT DESCRIPTION AND MODE OF OPERATION	5
4. DESIGN ASPECTS	6
4.1 Energy storage and switching circuit	6
4.1.1 Capacitors	6
4.1.2 Saturating reactor	7
4.1.3 Thyristor switch	7
4.1.4 Current monitoring	8
4.1.5 Pulse-matching autotransformer	9
4.2 Power converter for capacitor charging	9
4.2.1 Input autotransformer	9
4.2.2 d.c. chokes	11
4.3 Electronics, timing, and controls	11
4.3.1 Electronics and controls	11
4.3.2 Timing	12
5. TEST RESULTS	13
6. CONSTRUCTION	14
7. CONCLUSION	15
REFERENCES	15
APPENDIX A: Capacitor discharge section	16
APPENDIX B: Current-smoothing choke	18

List of figures

Fig. 1: Functional block diagram of the Li-lens pulser equipment

Fig. 2: Circuit diagram of the Li-lens pulser and power converter

Fig. 3: Gate structure of a switching thyristor*)

Fig. 4: Operating conditions of switching thyristors

Fig. 5: Voltage vector diagram and connections of the input autotransformer

Fig. 6: Mains voltage and autotransformer primary and secondary a.c. current waveforms

Fig. 7: Choke currents and total d.c. current

Fig. 8: Capacitor-charging current and voltage waveforms (the current pulse is due to the reverse capacitor voltage during discharge)

Fig. 9: Waveforms of Li-lens current I, switching-section current $I_{1,2,3}$, and capacitor voltage U_C at 1 MA

Fig. 10: Constructional layout of the charging power converter

Fig. A1: Simplified diagram of the Li-lens pulser and load

Fig. A2: Charging voltage U_o, current pulse rise-time T_p, and reverse capacitor voltage U_1 as a function of energy storage capacitance C with the autotransformer turns-ratio as the parameter

Fig. A3: Li-lens pulse current $I(t)$ and energy storage capacitor voltage $U(t)$

Fig. B1: Equivalent capacitor-charging circuit

Fig. B2: Applied rectifier voltage $U_R(t)$ and approximate shape of charging current I_C and capacitor voltage U_C

*) Courtesy of MEDL (UK)

List of tables

Table 1: Performance requirements

Table 2: Characteristics of energy storage capacitors

Table 3: Characteristics of the saturating reactors

Table 4: Characteristics of the autotransformer

Table A1: Basic design parameters

1. INTRODUCTION

Lithium lenses were originally developed at the Institute for Nuclear Physics (INP) in Novosibirsk (USSR) for the collection of positrons downstream from a production target.

The development was later pursued at FNAL (USA) and at CERN to obtain efficient $\bar{p}$ sources for large $\bar{p}p$ colliders.

A 36 mm diameter Li lens has been built at CERN, as a design scaled-up from a 20 mm FNAL/CERN lens [1], to be installed in the Antiproton Accumulator and Collector (AAC) downstream from the iridium target, with the aim of increasing the $\bar{p}$ yield by up to 40%.

The cylindrical Li lens forms the single secondary turn of a toroidal current stepping-up and impedance-matching transformer, which has been designed and built at INP, where there is considerable expertise in pulsed devices.

The matching transformer is powered by a capacitor discharge pulser and power converter. The pulser has been designed at CERN, following the decision in June 1988 to implement the Li-lens scheme for the AAC.

The equipment related to this project is shown schematically in Fig. 1.

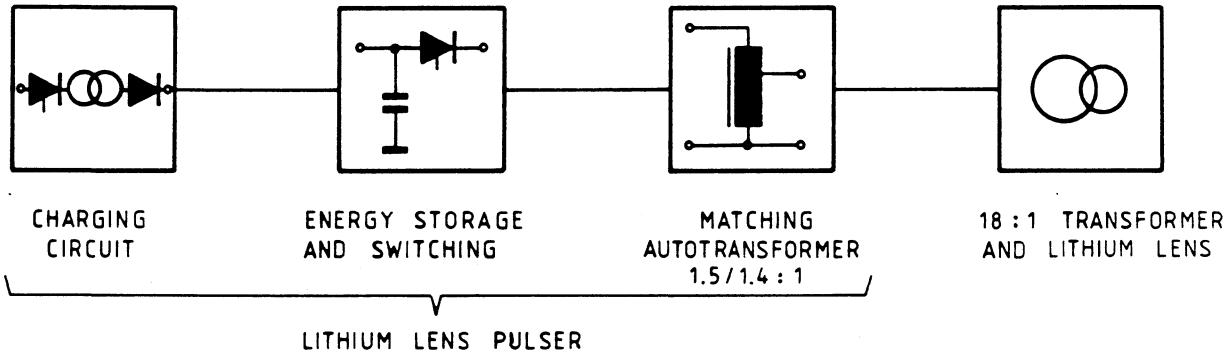

Fig. 1: Functional block diagram of the Li-lens pulser equipment

2. PERFORMANCE REQUIREMENTS

The aim of the pulser project was to achieve a current of 1 MA in the lens at 4.8 s repetition time in order to be able to carry out tests as soon as possible, and later to reach a current of 1.3 MA at 2.4 s operationally.

The pulser design was based on a lens impedance, given by its geometry, of resistance $R = 40\ \mu\Omega$ and inductance $L = 35$ nH.

The total load impedance, as seen at the output of the pulser and taking into account all elements of the installation as well as temperature and skin effects, was

assumed not to exceed $R = 22$ mΩ and $L = 16$ μH. The 18:1 turns-ratio of the toroidal lens transformer was imposed by INP. On account of the extremely tight time schedule and limited resources it was necessary to re-use, as far as possible, equipment that was already in service at CERN. In particular, a batch of 4.5 kV energy storage capacitors could be recuperated from a previous neutrino-experiment installation. This voltage fits well with the ratings of large thyristors currently available, and has led to the choice of a maximum capacitor charging voltage of 4.2 kV.

The other requirements for the Li-lens pulser are shown in Table 1.

Table 1
Performance requirements

Peak current (MA)	Current rise-time (ms)	Current pulse duration (ms)	Negative current (MA)	Pulse repetition period (s)	Pulse-to-pulse reproducibility (%)
1.3	1	< 3.5	< 0.01	2.4 or 4.8	0.5

3. CIRCUIT DESCRIPTION AND MODE OF OPERATION

The circuit principle of the Li-lens pulser and power converter, consisting of the pulse-matching autotransformer AT2, the energy storage and switching section, and the capacitor charging section, is shown in Fig. 2.

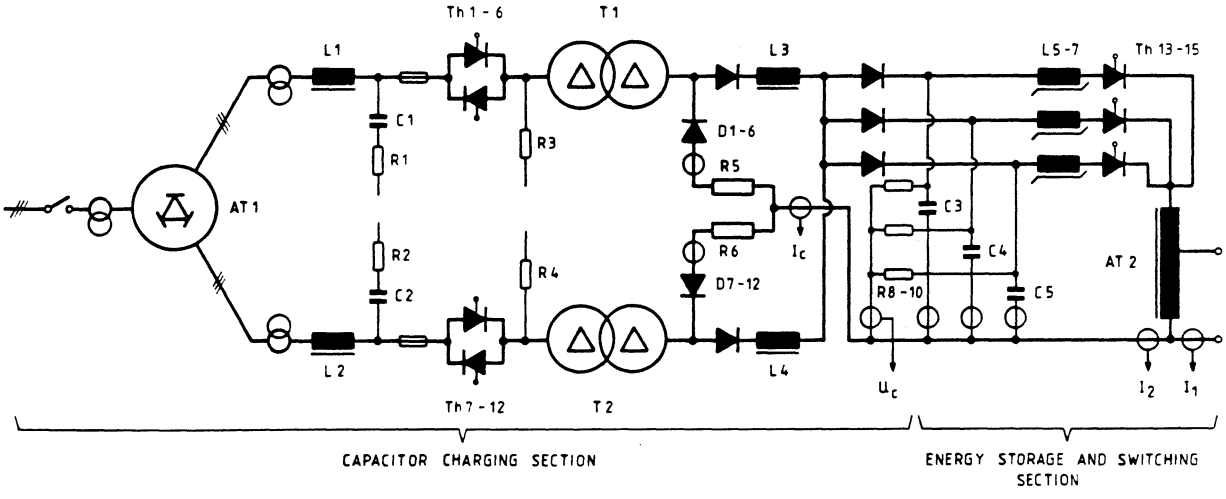

Fig. 2: Circuit diagram of the Li-lens pulser and power converter

The capacitor charging circuit is composed of an autotransformer (AT1), having two three-phase outputs shifted by 30° el, feeding two a.c. thyristor controllers (Th1–Th12) on the primary of two identical stepping-up transformers (T1 and T2). The HV sides of the transformers are connected in parallel via diode rectifiers (D1–D12) and decoupling chokes (L3 and L4).

Three separate capacitor banks are charged in parallel via decoupling diodes and switched simultaneously onto the primary of the pulse-autotransformer AT2 via di/dt limiting saturating reactors (L5–L7) and power thyristors (Th13–15).

The individual and the total charging current (I_C) as well as the capacitor voltage U_C are monitored by d.c. current transformers. The pulse current on each individual discharge circuit and on the secondary of the autotransformer AT2 are monitored by special transformers.

4. DESIGN ASPECTS

The circuit layout of the Li-lens pulser is straightforward; consequently, only a few interesting features and design aspects will be presented in more detail.

4.1 Energy storage and switching circuit

The selection of the circuit parameters is illustrated in Appendix A.

4.1.1 Capacitors

The capacitors used in the pulser were those that had in the past been specified and ordered for the Neutrino Experiment by the EF Division [2]. Their characteristics are given in Table 2.

Table 2
Characteristics of energy storage capacitors

Capacitance per unit (μF)	Number of units	Nominal voltage (kV)	Stored energy per unit (kJ)	Dielectric/ Impregnation/ Armatures	Dielectric stress at 4.5 kV (V/μm)	Design lifetime (pulses)	Make
200	108 3 × (3 × 12)	4.5	2	Paper (4) + polyethylene (1)/ Castor oil/ High-current Al foil	Paper: 21 Plastic: 40	2×10^7	AEROVOX (USA)

4.1.2 Saturating reactor

A di/dt limiting saturating reactor is connected in series to the HV thyristor in each of the three capacitor switching sections.

The characteristics of these reactors are collected in Table 3.

4.1.3 Thyristor switch

The thyristors are 75 mm amplifying gate units, type DCR–SU–1478 4545 [MEDL (UK)]. The structure of the gate and of the auxiliary thyristor, shown in Fig. 3, reduces spread-out distances on the silicon slice to less than 20 mm.

Table 3
Characteristics of the saturating reactors

Nominal inductance (μH)	Conductor/ Number of turns	Iron type/ Cross-section (cm^2)	Saturation current (A)	Nominal peak/r.m.s. current (kA)	Cooling	Make
100/10	Al/(2×6)	M6/32	1000	20/0.5	Natural-air convection	TRAFOMEC (Italy)

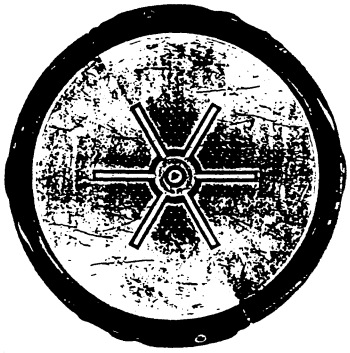

Fig. 3: Gate structure of a switching thyristor

The expression for the forward voltage drop of these thyristors is

$$U_d = [1.4 + 0.3 \times 10^{-3} \times I \text{ (A)}] \qquad \text{(in volts)} .$$

The surge non-repetitive 4 ms on-state sinusoidal current is given in the data sheets as 32 kA for an $\int i^2 \cdot dt$ of 4.2 $MA^2 \cdot s$.

The operating conditions of the thyristors in the Li-lens pulser are illustrated in Fig. 4.

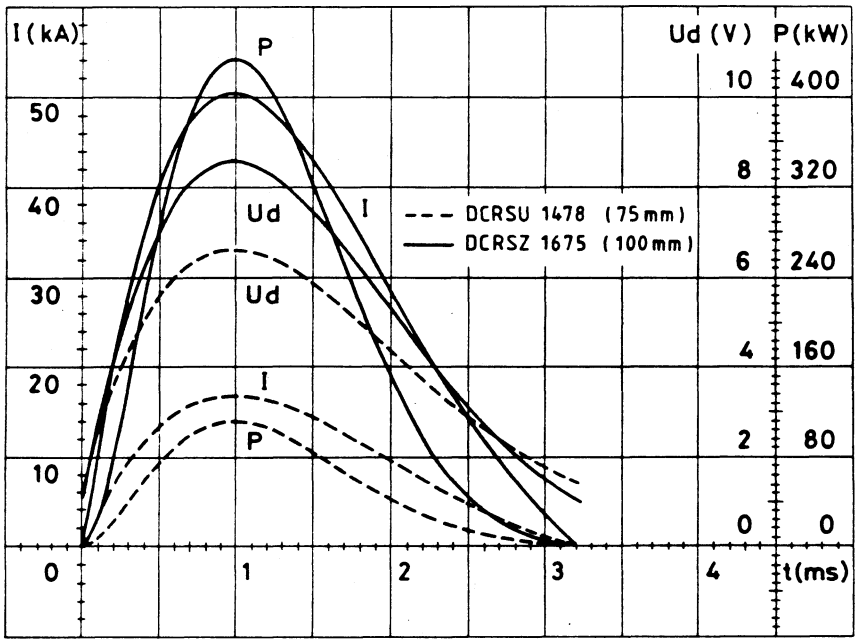

Fig. 4: Operating conditions of switching thyristors

Envisaging even more powerful applications, comparison is made with a 100 mm device, type DCR 1675, carrying a current pulse of 50 kA, and whose forward voltage drop has been assumed to be expressed as

$$U_d = [1.0 + 0.15 \times 10^{-3} \times I \text{ (A)}] \quad \text{(in volts)} \ .$$

The allowed repetitive peak thyristor current depends on the heatsink capability, which determines the initial junction temperature as a function of the mean losses. Taking this into account, an on/off time ratio of 4 ms/2.4 s, as at present, would allow 40 kA to pass in the 75 mm thyristor on a single-shot basis, and probably 70 kA in the 100 mm device.

The design and testing of a prototype switching unit with a 100 mm thyristor would certainly be of interest for future applications.

4.1.4 Current monitoring

The capacitor discharge current in each switching section is monitored by a type 1423 [Pearson (USA)] pulse current transformer to control the current sharing.

A 301X-type current transformer is used to monitor the total current on the secondary of the autotransformer AT2.

4.1.5 Pulse-matching autotransformer

A three-limb monophase autotransformer adapts the capacitor discharge circuit to the load in order to obtain the specified peak current and rise-time for a given maximum voltage (see Appendix A). Its magnetic circuit has been designed assuming that the working frequency be 125 Hz and that the $\int u \cdot dt$ be 5.35 V·s.

A distributed airgap allows operation with the voltage and current waveforms of a strongly damped capacitor discharge circuit, without the need for an auxiliary d.c. bias.

Minimum winding impedance is obtained by using a flat copper conductor and keeping the current density under 1 A/mm^2 for a total of 30 turns. The winding around the central core limb is divided into three layers of 10 turns each.

The interturn insulation is made with two Nomex sheets of 0.18 mm thickness. The windings are designed for a test voltage of 7 kV a.c. according to the IEC standards. Two outputs are foreseen at 20 and 21 turns, to cope with a possible inaccuracy of the assumed load impedance.

Some characteristics of the matching autotransformer AT2 are collected in Table 4.

Table 4
Characteristics of the autotransformer

Rating (MVA)	Primary voltage peak/ r.m.s. (kV)	Turns-ratio	Primary current peak/ r.m.s. (kA)	Secondary current peak/ r.m.s. (kA)	Air gap (mm)	Iron cross-section (mm^2)	Dimensions (ℓ × w × h) (m^3)	Weight (t)	Secondary impedance R/L (mΩ)/(μH)	Make
4.2	4.2/2.97	30/20 30/21	48/1.4 51/1.5	73/2.1	4	1200	0.8 × 0.96 × 1.6	3.5	0.2/1.4	TRASFOR (Switzerland)

4.2 Power converter for capacitor charging

The power converter has been manufactured in industry [OCEM (Italy)] following a CERN performance specification [3]. CERN has also contributed to its design.

4.2.1 Input autotransformer

An autotransformer with extended delta-winding feeding the thyristor controllers has been selected for reasons of magnetic balance and decoupling of 3rd order harmonics.

The phase connection and the vector diagram of this autotransformer are shown in Fig. 5.

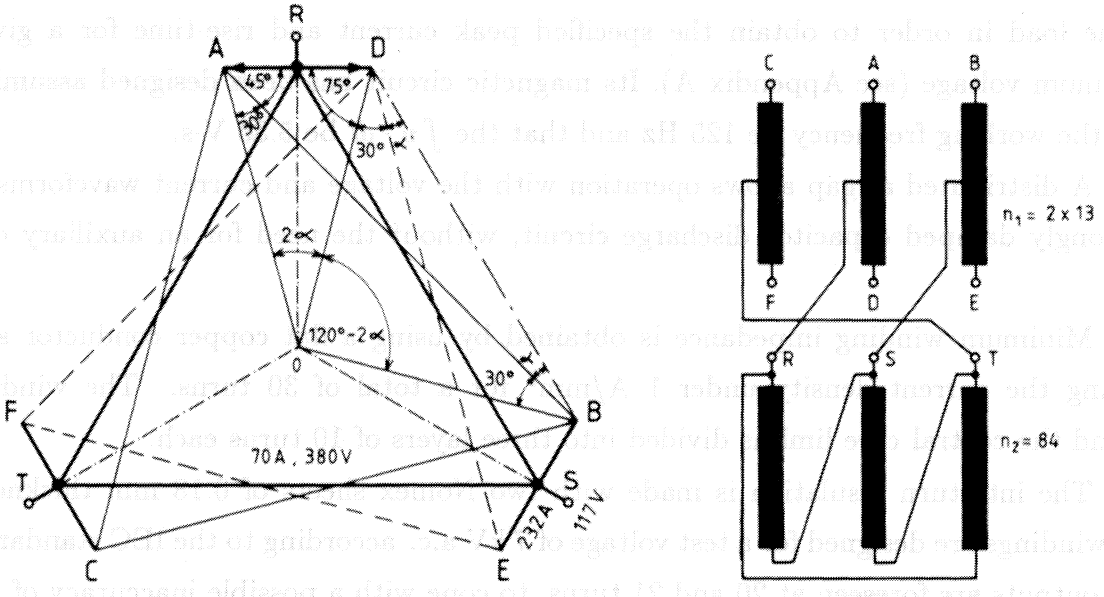

Fig. 5: Voltage vector diagram and connections of the input autotransformer

The desired phase shift $\alpha = \pm 15°$ is obtained by imposing a turns-ratio RS/AD $= \sqrt{3}/\ (2\ \mathrm{tg}\ \alpha) = 3.2320$.

The rating of the autotransformer is 81 kVA.

The operating conditions for this device are illustrated in Fig. 6, where the secondary phase-current waveform and the resulting primary a.c. line current are shown.

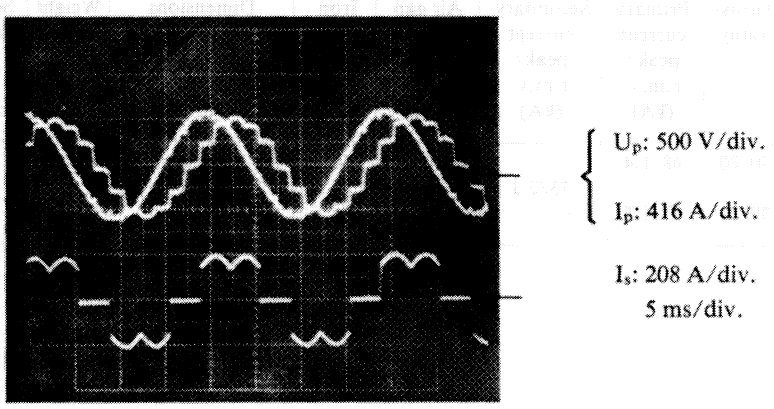

Fig. 6: Mains voltage and autotransformer primary and secondary a.c. current waveforms

In the case of this power converter, one can express the input active power P_1 and apparent power S_1—assuming a constant d.c. charging current I_C and disregarding freewheeling and losses—as follows:

$$P_1 = I_C \times U_C \qquad \text{and} \qquad S_1 = \sqrt{3} \times U_{line} \times I_{line} \ ,$$

where $I_{line} = k_1 \times I_C$ depends on the connection and turns-ratio of the transformers T1 and T2.

Under the above assumptions, the power factor of the converter, $\cos\phi = P_1/S_1$, which is of interest with respect to the effects on the mains, is therefore proportional to the output voltage U_C.

4.2.2 d.c. chokes

The a.c. filters and the thyristor controllers, as well as the stepping-up transformers and the rectifiers, have been designed according to the conventional criteria for this type of power converter.

Particular attention has been devoted to the design of the d.c. chokes, which fulfil the multiple function of paralleling the phase-shifted HV rectifiers, of smoothing the current to better than 10% for efficient charging, and of limiting the reverse discharge current through the rectifier.

On the basis of the design steps summarized in Appendix B, a value of 0.24 H has been selected for a mean d.c. rectifier current of 25 A.

The choke currents and the resulting d.c. current waveforms are shown in Fig. 7.

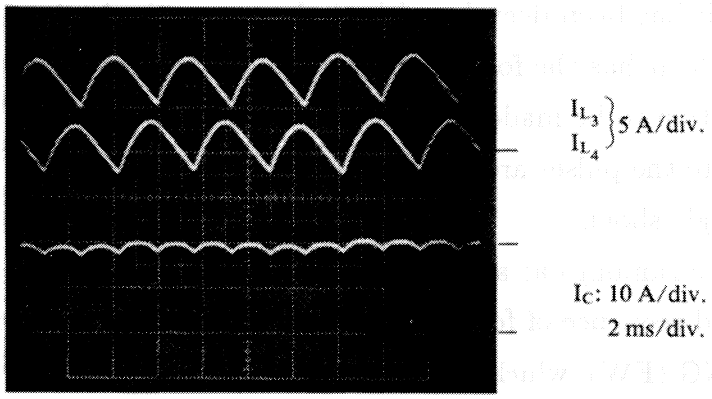

Fig. 7: Choke currents and total d.c. current

4.3 Electronics, timing, and controls

4.3.1 Electronics and controls

The electronics of the power converter is based on a number of industrial [OCEM (Italy)] printed-circuit boards (PCB), of 3U–L–Europe standard.

The most important PCBs are listed below:

- The voltage and current setting and the control PCB, consisting of two parallel servoloops working in sequence during the capacitor-charging and voltage-stabilization phase.
- The thyristor gate control PCBs, which produce six pulses of 120° duration at 60° intervals per period. The total firing delay with respect to the start of positive half-waves is the sum of the time delays of three cascaded timers, whose time is regulated by the control voltage. The firing pulse-power amplifiers and isolating transformers are located close to the thyristors.
- The interlock PCB, consisting of a number of digital modules that detect and memorize the fault signals.
- The timing PCB, which is described in the next paragraph.

To avoid noise problems, all timing signals entering or leaving the power converter are galvanically isolated.

The remote-control and external interlock electronic circuits have been built at CERN and are located in a separate central system-supervisory rack. This plays the role of interface between the pulser, the Li-lens and its auxiliaries, the central timing, and the computer control, and supervises the safety aspects of the whole installation.

4.3.2 Timing

The timing PCB has been deeveloped by industry on the basis of a performance specification by CERN. It has the following features:

i) It allows a selection to be made between three modes of operation:
- REMOTE, where the pulses are controlled by the external central timing system;
- LOCAL SS (single shot);
- LOCAL FR (free running) at a repetition period of 2.4 or 4.8 s.

ii) It creates a fixed sequence of four pulses on separate outputs, namely:
- FOREWARNING (FW), which starts the capacitor charge;
- WARNING (W), which interrupts the voltage stabilization phase and makes the power converter safely ready for discharge;
- START (ST), which triggers the capacitor discharge thyristors;
- MEASURE (MEA), which triggers the S/H circuit to measure the current in the Li-lens when the beam crosses it.

iii) It assures that the operating cycle of the power converter is always initiated by a FW pulse. Assuming that the operation is REMOTE, once the cycle has started it would in any case be terminated by internal safety pulses if any external pulse were missing.

iv) It causes any timing pulse, once accepted, to inhibit its own entry and to make the way free for the next one in the sequence. The modular-principle solution implies starting two cascaded counters for each pulse of the sequence: the first counter closes the way to any other pulse, the second one opens a time window where the next pulse can enter. If this pulse is missing, then the end of the time window generates a substitute safety pulse to continue the sequence. Therefore a minimum charging-time as well as a minimum converter blocking-time before discharge are assured.

This technical solution for the Timing PCB guarantees that the operating conditions of the pulser are well defined, that all precautionary steps are taken (i.e. blocking the gate control, setting the reference signals to zero, resetting the servoloop integrators, etc.), and that the HV capacitors are not kept unduly charged for any length of time. This helps to achieve high equipment reliability, safe operation, and easy signal monitoring during commissioning and repair.

5. TEST RESULTS

Some waveforms observed during Li-lens tests, with an autotransformer turns-ratio of 30/20, are shown in Figs. 8 and 9.

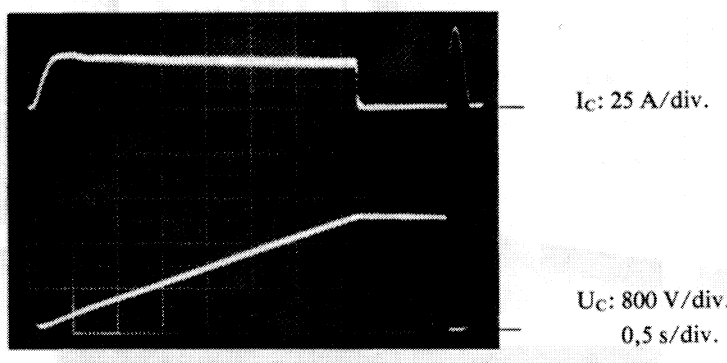

Fig. 8: Capacitor-charging current and voltage waveforms (the current pulse is due to the reverse capacitor voltage during discharge)

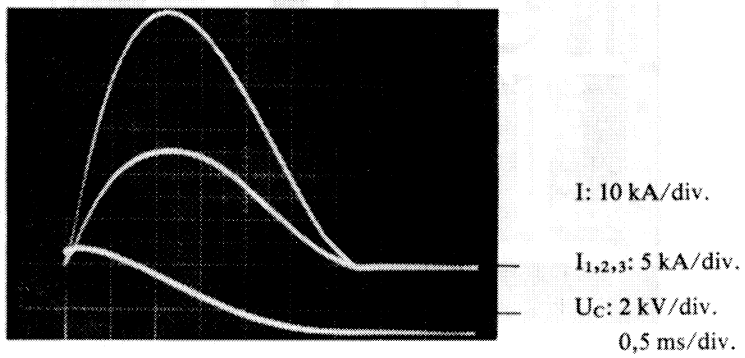

Fig. 9: Waveforms of Li-lens current I, switching-section current $I_{1,2,3}$, and capacitor voltage U_C at 1 MA

The Li lens has been pulsed at a current up to 1.2 MA and at 4.8 s repetition time with an autotransformer turns-ratio of 30/15. In the course of this first test, the end flange of the lens did not withstand the electromagnetic constraints and was permanently deformed.

Once the flange design was modified, the tests were resumed, in July 1989, with an autotransformer turns-ratio of 30/21.

Finally, the lens was put into the beam for a short time and operated at 1.1 MA to demonstrate the design $\bar{p}$ yield enhancement factor of 1.4.

The pulser has been used since September 1989 for duration and development tests of the lens and its toroidal transformer.

6. CONSTRUCTION

The layout of the charging power converter is shown in Fig. 10.

It consists of three cubicles containing

i) the a.c. input circuit, the autotransformer, the two a.c. filters, and, in the upper part, the electronics crates;

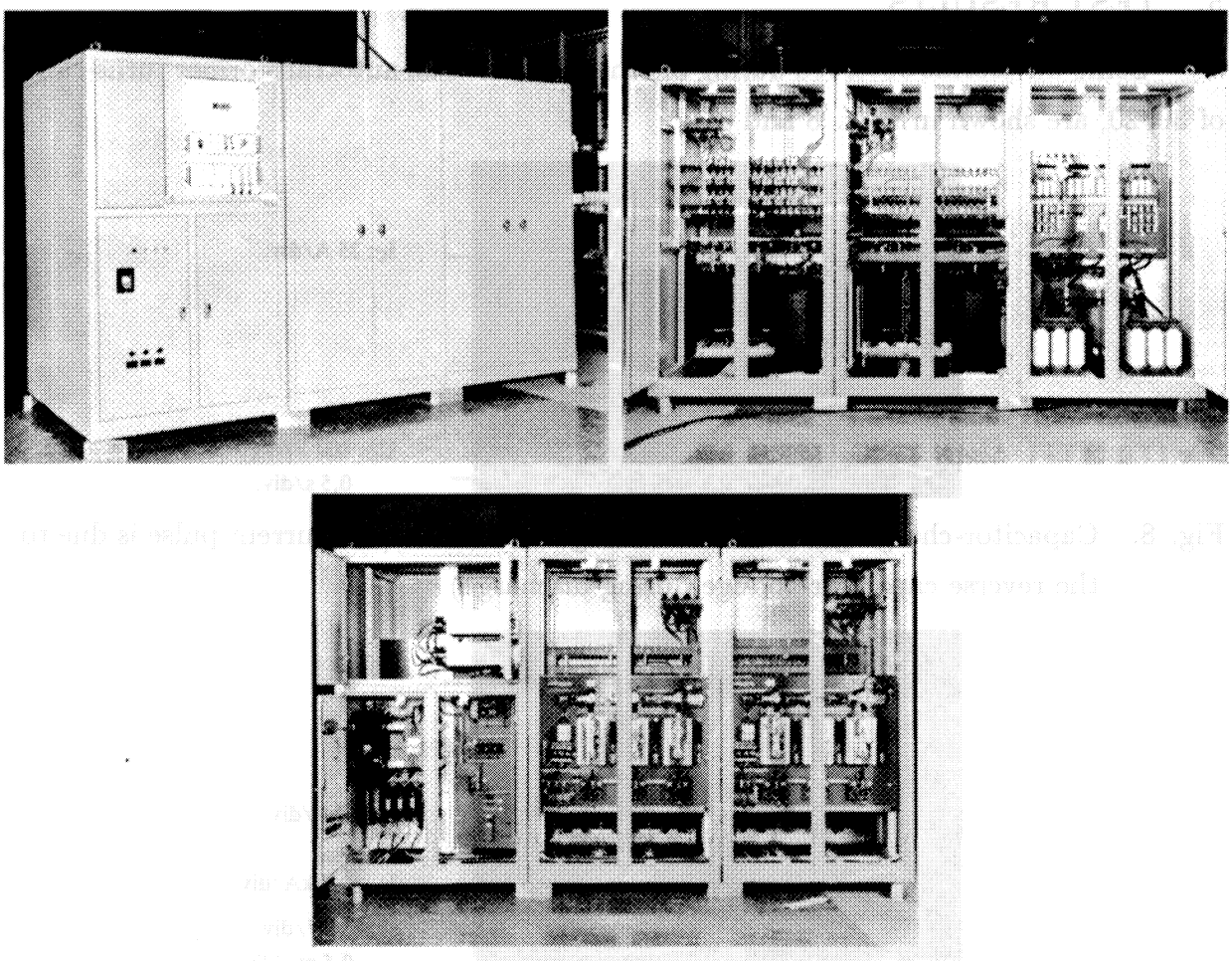

Fig. 10: Constructional layout of the charging power converter

ii) and iii) the two a.c. thyristor controllers, the transformers, the rectifiers, and the HV circuits, each set in a separate cubicle.

The overall dimensions of the converter cubicles are 1.2 $\times$1.5 $\times$ 2.1 m^3.

7. CONCLUSION

The 200 kJ Li-lens pulser has been successfully produced and commissioned within an extremely tight time-schedule and with very few resources.

It includes one of the most powerful power converters of this type (50 A; 4.2 kV) so far designed and built completely by industry—power part and electronics—on the basis of a concise CERN performance specification.

The success of this project is the result of the engineering expertise existing at CERN and of the design and manufacturing competence in European industry.

Acknowledgements

The enthusiasm and involvement of all those who participated in the factory testing and in the final commissioning of the pulser at CERN are greatly appreciated.

REFERENCES

[1] R. Bellone, D. Fiander, J. Hangst, P. Sievers and G. Silvestrov, "Performance and operational experience with CERN lithium lenses", Proc. European Particle Accelerator Conf., Rome, 1988, ed. S. Tazzari (World Scientific, Singapore, 1989), Vol. 2, p. 1401.

[2] R. Grüb, Technical specification for the energy storage capacitors of the 1.2 MJ pulse system for the narrow-band neutrino beam in the West Area, CERN/D.Ph.II/Beam Tech/Int. Note 73–16 (1973) (Revised March 1974).

[3] G. McMonagle, Technical specification for a capacitor recharging power supply, CERN/PS/AR/SPEC 88–1 (1988).

APPENDIX A
CAPACITOR DISCHARGE SECTION

With reference to Fig. A1, the basic parameters for the design of the energy storage and switching section are summarized in Table A1.

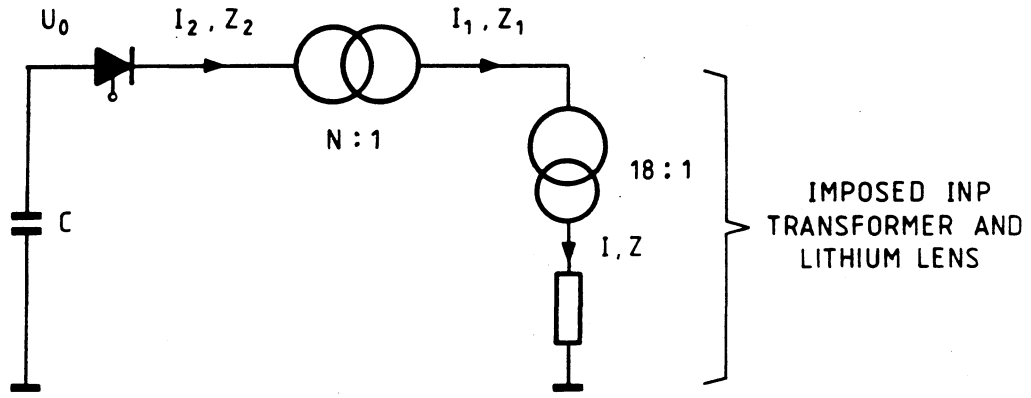

Fig. A1: Simplified diagram of the Li-lens pulser and load

Table A1
Basic design parameters

Peak pulse current I/I_1 (kA)	Pulse rise-time T_p (ms)	Charging voltage U_0 (kV)	Turns-ratio N	Duty cycle T_{ch}/T_{rep} (s)	Impedances R/L (mΩ/μH)	
1300/73	1 ± 0.10	⩽ 4	1 < N ⩽ 2	2/2.4	Z_1: 22/16	Z: 0.04/0.035

The diagram shown in Fig. A2 leads to the choice of a total energy storage capacitance of 21.6 mF—subdivided into three sections, each having 36 capacitors of 200 μF—and of an autotransformer turns-ratio of $1.4 < N < 1.5$ (finally, $N = 1.428$).

The Li-lens pulse current and the capacitor voltage waveforms, I(t) and U(t), as a function of time, computed according to the above choice of parameters, are shown in Fig. A3.

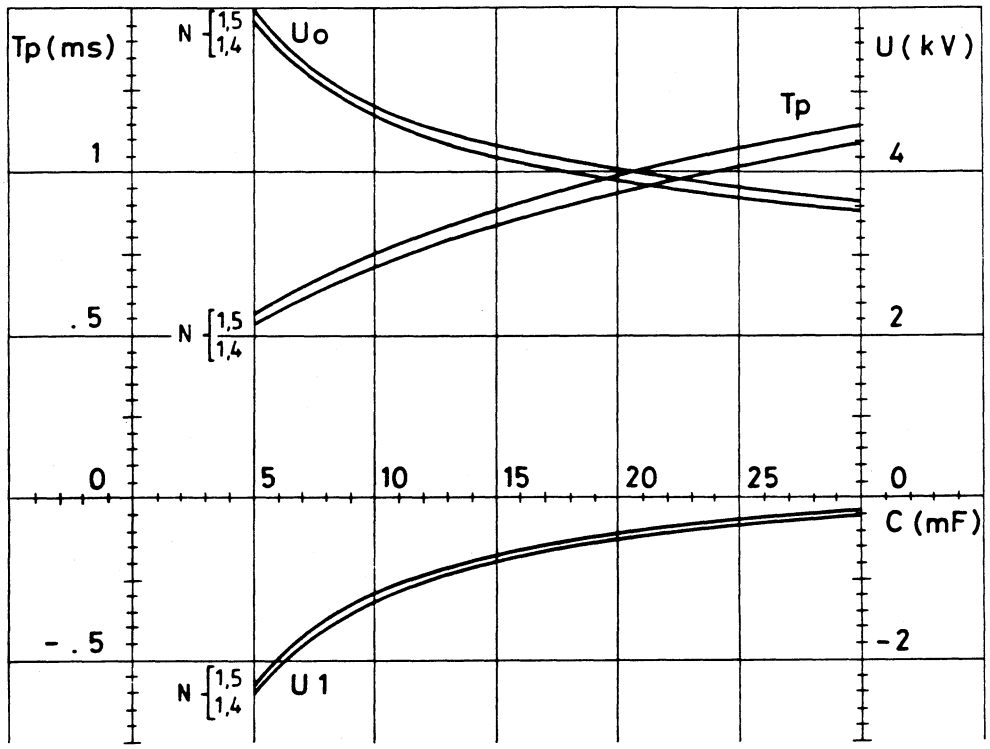

Fig. A2: Charging voltage U_o, current pulse rise-time T_p, and reverse capacitor voltage U_1 as a function of energy storage capacitance C with the autotransformer turns-ratio as the parameter

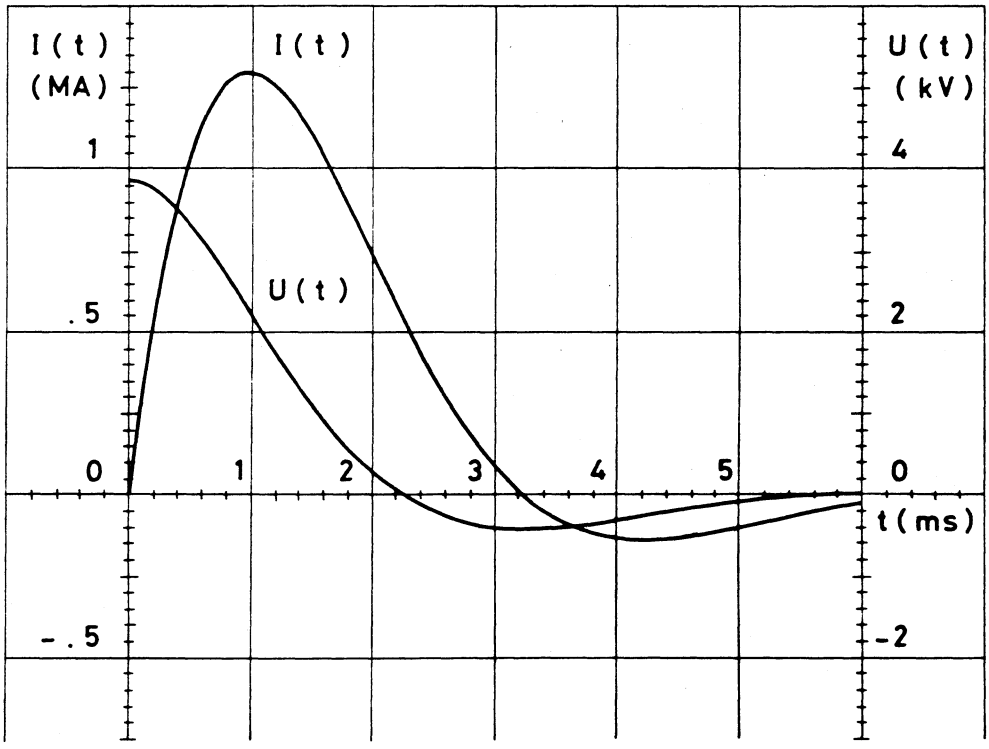

Fig. A3: Li-lens pulse current $I(t)$ and energy storage capacitor voltage $U(t)$

APPENDIX B
CURRENT-SMOOTHING CHOKES

Each HV rectifier is designed to deliver a d.c. current of 25 A average, with a maximum peak-to-peak ripple of 10%.

The waveform of the charging current has been computed as a function of time, with the choke inductance as the parameter, on the basis of the equivalent circuit shown in Fig. B1.

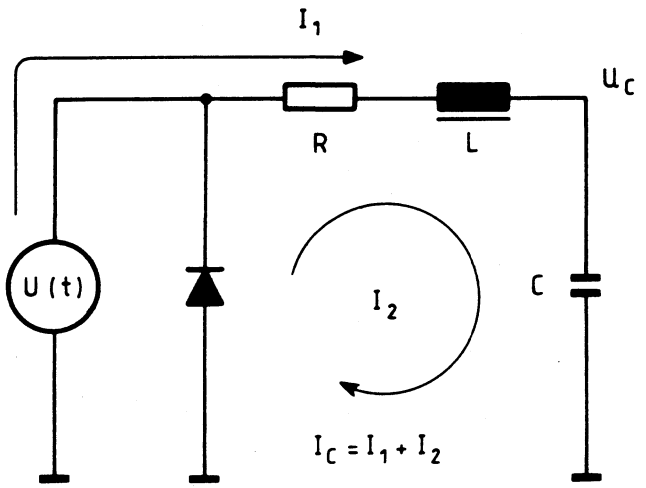

Fig. B1: Equivalent capacitor-charging circuit

Two modes of operation are considered:

i) the applied rectifier voltage $U_R(t)$ exceeds the instantaneous capacitor voltage U_C and energy is delivered from the mains;

ii) the capacitor voltage becomes higher than the rectifier voltage, and the energy stored in the choke drives a freewheeling current through the rectifier.

For both modes of operation, the circuit equations are solved with the proper initial conditions, assuming that cosinusoidal voltage sectors are applied: $U_R(t) = \hat{U} \cdot \cos(\omega t + \phi)$, with $\phi = (\pi/2) - \beta$, as shown in Fig. B2.

The circuit equation

$$R[i(t)] + L\left[d\frac{i(t)}{dt}\right] + \frac{1}{C}\int i(t)dt = U(t)$$

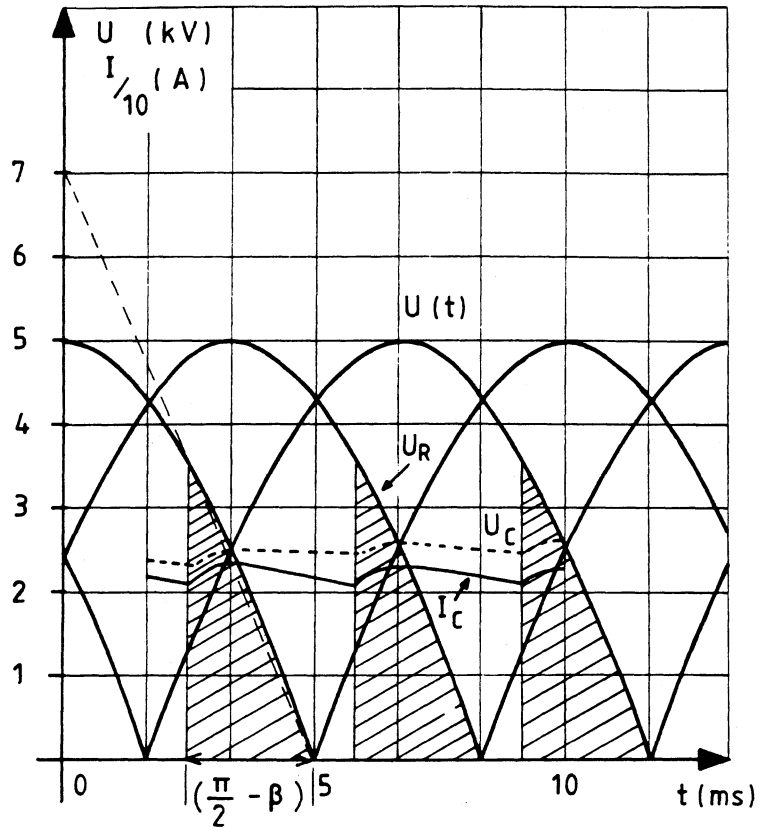

Fig. B2: Applied rectifier voltage $U_R(t)$ and approximate shape of charging current I_C and capacitor voltage U_C

is solved by applying the Laplace transform to obtain the expression of the current as a function of time for two situations:

i) when $U_R(t)$ exceeds U_C (assuming initial values I_{01}, U_{01}):

$$i_1(t) = \frac{1}{[(\omega_0^2 - \omega^2)^2 + 4\delta^2\omega^2]^{1/2}} \left\{ \frac{\hat{U}\cos\phi}{L} \left[\omega \sin\ (\omega t + \psi_1) + \frac{\omega_0^2}{\omega_1}\ \mathrm{e}^{-\delta t} \sin\ (\omega_1 t + \psi_2) \right] \right.$$
$$\left. - \frac{\hat{U}\sin\phi}{L} \left[\omega \sin\ (\omega t + \psi_3) + \frac{\omega_0\omega}{\omega_1}\ \mathrm{e}^{-\delta t} \sin\ (\omega_1 t + \psi_4) \right] \right\}$$
$$+ I_{01}\ \bar{\mathrm{e}}^{\delta t} \frac{\omega_0}{\omega_1} \sin\ (\omega_1 t + \psi_5) - \frac{U_{01}}{L\omega_1}\ \mathrm{e}^{-\delta t} \sin\ \omega_1 t;$$

ii) when $U_R(t)$ becomes smaller than U_C and current freewheeling takes place (assuming initial values I_{02}, U_{02}):

$$i_2(t) = I_{02}\ \mathrm{e}^{-\delta t} \left[\left(\cos\ \omega_1 t - \frac{\delta}{\omega_1} \sin\ \omega_1 t \right) - \frac{U_{02}}{I_{02}\omega_1 L} \sin\ \omega_1 t \right],$$

where ω is the frequency of the applied voltage $\dot{U}(t) = \hat{U} \cos\ (\omega t + \phi)$

$$\omega_0 = \frac{1}{\sqrt{LC}} \ , \qquad \delta = \frac{R}{2L} \ , \qquad \omega_1 = \sqrt{\omega_0^2 - \delta^2} \ ,$$

$$\psi_1 = -\text{arctg}\left(\frac{2\delta\omega}{\omega_0^2 - \omega^2}\right) \ ,$$

$$\psi_2 = \pi + \text{arctg}\left(\frac{-2\delta\omega_1}{\delta^2 - \omega_1^2}\right) - \text{arctg}\left(\frac{-2\delta\omega_1}{\delta^2 - \omega_1^2 + \omega^2}\right) \ ,$$

$$\psi_3 = \text{arctg}\left(\frac{-X}{R}\right) \ , \qquad X = \left(\omega L - \frac{1}{\omega C}\right) \ ,$$

$$\psi_4 = \pi + \psi_5 - \text{arctg}\left(\frac{-2\delta\omega_1}{\delta^2 - \omega_1^2 + \omega^2}\right) \ ,$$

$$\psi_5 = \pi + \text{arctg}\left(\frac{-\omega_1}{\delta}\right) \ .$$

The capacitor voltage $U_C = [(1/C) \int i(t)\ dt + U_{0i}]$ is obtained by integrating the current function, but the lengthy voltage expressions are not written down here.

On the other hand, the smoothing choke extends in time and limits in amplitude the backswing current produced by the negative capacitor voltage at the end of the discharge. It also plays the role of an interphase reactor for parallel operation of the HV rectifiers.

An inductance L = 0.24 H has been selected in order to satisfy these different requirements (see also subsection 4.2.2).